CAN A MICRO-PULSE LIDAR MEASURE RAMAN NITROGEN SIGNALS FROM THE ATMOSPHERE?

T.A. Berkoff[(1)], E. Welton[(2)], J. Spinhirne[(2)]

[(1)]*University of Maryland Baltimore County, NASA GSFC Code 613.1, Greenbelt, Maryland 20771 USA*
[(2)]*NASA Goddard Space Flight Center, Code 613.1, Greenbelt, Maryland 20771 USA*

ABSTRACT

An elastic scattering atmospheric measurement at 523 nm was obtained using a Micro-Pulse Lidar (MPL) system with a transmitted laser beam that was attenuated to simulate the expected signal from Raman scattering due to atmospheric Nitrogen. Results show the expected performance if an MPL was modified to detect a second wavelength near 596 nm, corresponding to the Nitrogen Raman-shifted wavelength. Despite the MPL small receiver size and low energy, experimental results suggest this power-aperture combination may be sufficient to detect Raman Nitrogen signals greater than 6 km in altitude at nighttime, when background light levels are low.

1. INTRODUCTION

Developed by NASA Goddard Space Flight Center in the early 1990's, Micro-Pulse Lidars (MPLs) are single-channel elastic scattering systems [1] that have been utilized at a wide variety of remote field locations. These systems are currently operating at multiple sites around the globe as part of the Micro-Pulse Lidar Network (MPLNET) to monitor atmospheric aerosols and clouds on a continuous, multi-year basis[2]. Unlike many lidar systems used for aerosol monitoring, MPLs are unique due to the "eye-safe" (Class II) transmitted energy and small size. Signal-to-noise performance is optimized through the use of a high repetition rate laser, narrow field-of-view, and narrow band-pass filters. Figure 1 shows a photograph and optical component details of the MPL system.

Also for many years, the use of Raman backscattering in larger-scale lidar systems has demonstrated its utility for retrieval for water vapor and aerosol extinction profiles[3]. These systems typically emit laser light in the ultra-violet range and measurements using the Raman shifted wavelengths for atmospheric Nitrogen (N_2), oxygen, water vapor, and liquid water have been demonstrated [4]. For aerosol retrievals, a key advantage of the use of Raman scattering from atmospheric N_2 allows for a more direct retrieval of aerosol extinction that ordinarily cannot be achieved by elastic scattering measurements alone. However, Raman scattering is a weak inelastic process, with cross-sections orders of magnitude smaller than corresponding rayleigh elastic scattering signal returns. Consequently, many systems described to date rely on large-size diameter receivers (> 0.3 meters) and large pulse-energy laser sources (50 mJ/pulse) to overcome the inherent low-level signal returns. These configurations are not typically eye-safe at the transmission output. These factors limit their use in networks like MPLNET, where small size, unattended operation, eye-safety, and low cost are dominant factors for implementation.

Current operational algorithms used in MPLNET rely on co-located sunphotometer measurements of aerosol optical depth as a boundary constraint to find the layer-average extinction-to-backscatter (S) ratio[5]. Non-homogeneous changes in the S-ratio within a layer will contribute to an error in retrieved extinction profile shape. Various closure studies have been conducted over the years, comparing Raman and airborne sun-tracking photometer measurements to MPL extinction retrievals [6,7]. From these studies, general agreement were noted for most of the extinction data, however exceptions were observed. Additionally, sunphotometry measurements are not available at night, thus MPLNET nighttime optical calibration factors are interpolated from daytime measurements, introducing a potential source of error for nighttime extinction retrievals.

In this study, the ability of a MPL to measure Raman-shifted N_2 backscatter returns from the atmosphere was investigated for nighttime measurements. Although a MPL was never intended to obtain Raman backscatter measurements, the incorporation of N_2 measurements into an MPL would extend capabilities for nighttime calibrations and aerosol extinction retrievals.

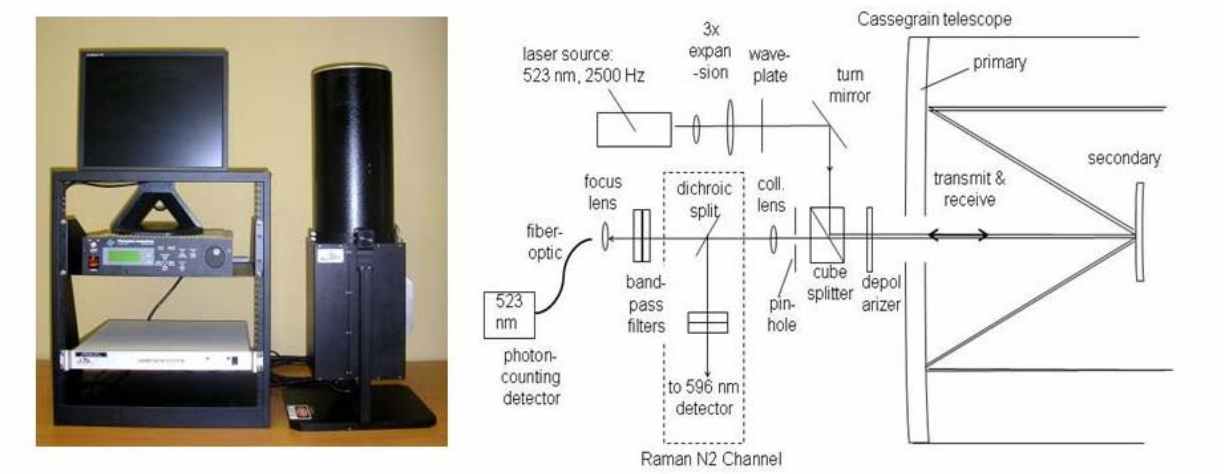

Fig. 1. (a) Left: Photograph of a MPL system (courtesy of Sigma Space). **(b) Right:** Optical layout of an MPL transceiver components. Dashed box shows where a Raman N_2 channel could be added by incorporation of a dichroic mirror in the existing receiver path.

2. ANALYTICAL DESCRIPTION

The experimental simulation described here relies on the attenuation of the MPL transmitted laser signal to simulate the expected signal return due to Raman N_2 atmospheric backscatter. The range dependent lidar signal for a Raman N_2 backscatter signal can be represented by

$$S(r) = A \cdot E \cdot \beta_{N2}(r) \cdot T_e(r) \cdot T_{N2}(r) \qquad (1)$$

where E is the transmitted energy, r is the distance of the scattering source to the lidar, $\beta_{N2}(r)$ is the backscatter from Raman-shifted atmospheric N_2, $T_e(r)$ is the forward transmission loss of the laser light to the scattering source, $T_{N2}(r)$ is the return transmission loss at the Raman N_2 shifted wavelength, and A is a value representing a combination of usual instrumental corrections including range-squared normalization and overlap correction.

The relationship between the Raman N_2 and Rayleigh signal magnitudes can be estimated from the backscatter cross-section and number density terms. Reported backscatter differential cross-sections for Rayleigh and Raman N_2 are σ_e=4 x 10^{-27} cm^2/sr and σ_{N2}=3 x 10^{-30} cm^2/sr respectively[8]. Accounting for the cross-sectional differences, and since N_2 atmospheric fractional number density is ~0.8, Raman N_2 backscatter magnitude can be estimated from

$$\beta_{N2}(r) = 0.8 \cdot \frac{\sigma_{N2}}{\sigma_e} \cdot \beta_e(r) \qquad (2)$$
$$= 6x10^{-4} \cdot \beta_e(r)$$

where $\beta_e(r)$ is the Rayleigh backscatter term. For an elastic transmission of an MPL at 523 nm, the Raman-shifted signal for N_2 will occur at ~ 596 nm. By approximating transmission properties at these two different wavelengths as $T_e(r) \sim T_{N2}(r)$ and substitution (2) into (1) yields

$$S(r) = A \cdot E \cdot 6x10^{-4} \cdot \beta_e(r) \cdot T_e(r)^2 \qquad (3)$$

This expression represents an equivalent magnitude signal for Raman N_2 based on Rayleigh observations, the key difference being the scaling constant of $6x10^{-4}$. Since transmitted energy term E is also a proportional scaling constant to $S(r)$, a simulation of a Raman N_2 signal magnitude can be accomplished by reduction in lidar energy E to match this scaling constant. It is important to note that (3) does not account for Mie scattering properties, and simulated Raman N_2 magnitudes obtained from elastic signal measurements should be considered only for particle-free sections of the profiles. Additionally, the $T_e(r) \sim T_{N2}(r)$ assumption will serve to underestimate actual Raman N_2 return magnitudes to some degree, since atmospheric transmission will be marginally higher at the longer 596 nm wavelength.

3. EXPERIMENTAL SIMULATION

Based on the information in Section 2, MPL experimental measurements at 523 nm were obtained at NASA GSFC to simulate the signal return for Raman-shifted atmospheric N_2. Initially, vertical profiles at 75 meter vertical and 1 minute time resolution were recorded with an MPL in its normal energy level emitting ~ 8.5 uJ/pulse at a repetition rate of 2500 Hz.

Figure 2 shows the MPL normalized relative backscatter (NRB) image obtained on May 23 from 2:05 to 2:30 UTC. This result incorporates the standard MPL instrumental corrections [9] (darkcount, deadtime, afterpulse, background subtract, and range-squared normalization) with the exception of the overlap function. At the time of this measurement the overlap function for this instrument had not been determined and is not needed for this study. The overlap effect is the characteristic loss in signal in the near range (0-6 km for an MPL) due to field of view vignetting losses as can be seen by the increased loss in signal when approaching the surface in the data.

Intermittent cirrus at 12 km were present during measurements; however, the lower-atmosphere temporal characteristics were relatively stable, including the dominant aerosol feature at 2 km. Based on AERONET[10] Level 2 (cloud screened and quality assured) sunphotometer results ~ 3.5 hours earlier, columnar aerosol optical depths were 0.23 and 0.18 for 523 nm (elastic) and 596 nm (Raman N_2) wavelengths respectively. A profile average from 2:25 to 2:30 UTC is presented in Figure 3(a). This profile was scaled to match the 9-11 km particle-free region to a U.S. standard atmosphere model Rayleigh signal attenuated by an aerosol optical depth of 0.2. The model comparison shows good agreement with the predicted Rayleigh slope decay at high altitudes and also helps assess the boundary layer transition to the particle free portion of the atmosphere.

After the initial measurements at normal energy levels, the laser output for the MPL was attenuated with a neutral density filters reducing the MPL output by 3 $x10^{-4}$, to an energy level of ~3 nJ/pulse. This level of attenuation is ~ 2 times larger than indicated in Section 2, and therefore results are expected to conservatively represent the actual performance of a real Raman N_2 signal. Vertical profiles were recorded for 20 minutes from 2:36 to 2:56 UTC, and the resultant profile average is presented in Figure 3(b). This profile has the same basic response shape as the non-attenuated case, but with excess noise due to the reduction in energy.

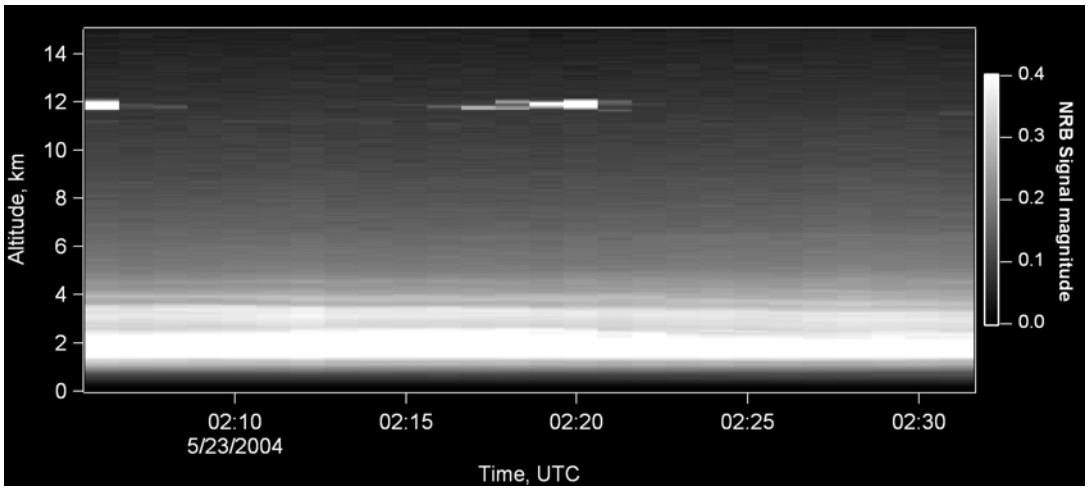

Fig. 2. MPL Lidar NRB image (overlap correction not applied) obtained from 2:05 to 2:30 UTC on May 23 at normal energy levels. The atmosphere is relatively stable with the exception of intermittent cirrus at 12 km.

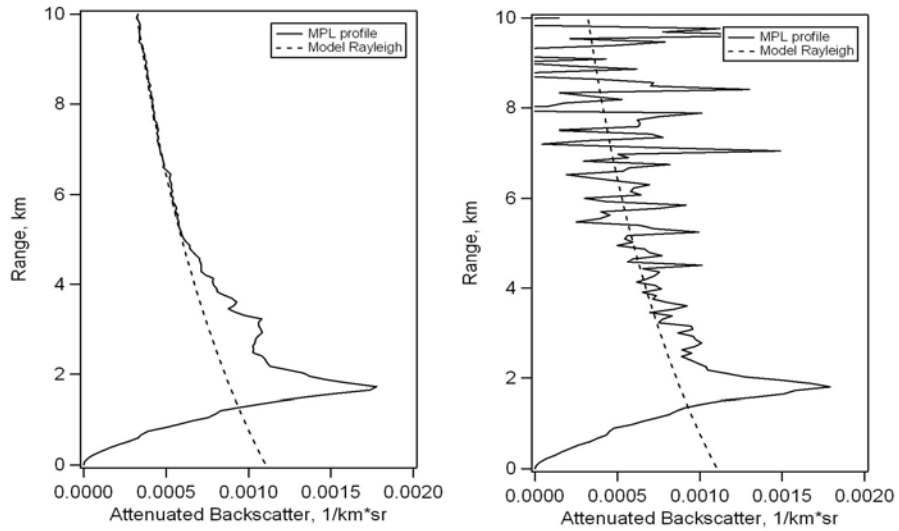

Fig. 3a (left) &b (right). MPL lidar NRB profiles (solid line, overlap correction not applied) for a five minute average at 8.5 uJ/pulse (left) and subsequent 20 minute average with energy reduced to ~ 3 nJ/pulse, representing an equivalent Raman N_2 signal (right). In both plots, model Rayleigh atmosphere is represented by the dashed lines.

Despite the magnitude of the noise present in Figure 3(b), return signals are clearly apparent at the 4-6 km range, where the profile is dominated by Rayleigh scattering. As a result, this is an indicator of the expected signal-to-noise for these altitudes for a Raman N_2 signal generated by an MPL operating at normal energy levels. Analysis of the raw signal counts indicate background light and afterpulse contributions had a negligible influence, with the observed signal being entirely dominated by detector dark counts (~80 Hz) for altitudes greater than 8 km.

4. SUMMARY AND CONCLUSIONS

Results obtained from an experimental simulation of a Raman backscatter signal indicate it is possible a Micro-Pulse Lidar system can obtain measurements of atmospheric N_2 at nighttime. For a 20 minute average and 75 meter vertical resolution, observed noise levels indicate that a Raman N_2 signals could be detected at altitudes as high as 6 km. Although actual Raman measurements were not obtained in this study, a future modification to the MPL receiver path could permit simultaneous Raman N_2 measurements and not interfere with existing MPL elastic measurement capabilities and operation. While measurements could only be obtained at nighttime when background levels are minimized, the additional measurement capability could prove useful for future lidar calibrations and retrievals of aerosol extinction.

5. ACKNOWLEDGEMENTS

The authors gratefully acknowledge financial support from the NASA Micro-Pulse Lidar Network (MPLNET) funded by the NASA Earth Observing System and Radiation Sciences Programs.

6. REFERENCES

1. Spinhirne, J.D, IEEE Transactions on Geoscience and Remote Sensing, 31, pp. 48-55, 1993.
2. see: mplnet.gsfc.nasa.gov
3. J.E.M. Goldsmith, et. al., Applied Optics, 37, 4979, 1998.
4. D.N. Whiteman et. al., J. Geophys. Res., 106, pp. 5211-5225, 2001.
5. E.J. Welton et. al., in Lidar Remote Sensing for Industry and Environmental Monitoring, Proc. SPIE, 4153, 151-158, 2001.
6. F. Russo et. al.,, Proc. International Laser Radar Conference, pp.599-602, 8-12 July 2001.
7. B. R. Schmid, et. al, *J. Geophys. Res.*, 111, D05S07, doi:10.1029/2005JD005837, 2006.
8. R. Measures, Laser Remote Sensing, John Wiley & Sons, New York, 1984.
9. J.R. Campbell et. al. *J. Atmos. Oceanic Technol.*, 19, 431-442, 2002.
10. see: aeronet.gsfc.nasa.gov